

Original Research

Conical Chitosan Conduits Combined With Methylcobalamin for Sciatic Nerve Transposition Repair

Qicheng Li^{1,2,†}, Fengshi Zhang^{1,2,†}, Shiyan Liu³, Yusong Yuan^{4,*}, Yuhui Kou^{1,2,5,*}

Submitted: 8 January 2025 Revised: 24 March 2025 Accepted: 16 April 2025 Published: 24 June 2025

Abstract

Background: The repair technology of peripheral nerve injuries has made great progress, but the simultaneous repair and promotion of nerve regeneration in multiple distal nerves remains a challenging task. The current cylindrical nerve conduits are unsuitable for nerve transposition repair. This study aims to assess the effect of conical chitosan conduits (different inner diameters at both ends) on nerve transposition repair, in conjunction with methylcobalamin (MeCbl). **Methods**: In this study, a conical chitosan conduit was used to bridge a 2 mm defect between the proximal common peroneal nerve and distal tibial nerve and common peroneal nerve in rats. Additionally, we administered MeCbl at various concentrations to evaluate post-surgical adjuvant treatment effect. At 16 weeks post-surgery, gait analysis, electrophysiology testing, transmission electron microscopy (TEM) observation, toluidine blue staining, immunofluorescence staining, muscle wet weight determination and Masson's trichrome staining were performed to assess nerve regeneration and reinnervation of gastrocnemius. **Results**: Gross observations did not reveal the formation of neuromas after bridging the distal nerves in each group. In terms of motor function (**p < 0.01), compound muscle action potential (CMAP) amplitude and latency (**p < 0.01), the quantity of regenerated nerve fibers, muscle fiber morphology and other parameters (**p < 0.01), 200 µg/kg MeCbl administration as a supplementary treatment had a significant positive impact compared to the chitosan conduit+normal saline (Chi/NS) group. **Conclusions**: Our findings demonstrated that conical chitosan conduits combined with MeCbl can effectively promote nerve transposition repair following multiple distal nerve injuries.

Keywords: chitosan; methylcobalamin; nerve regeneration; peripheral nerve injury; transposition repair

1. Introduction

Peripheral nerve injuries (PNI) present a significant challenge in regenerative medicine, often resulting in severe functional impairments and a reduced quality of life. Among these injuries, conditions such as long-distance nerve defects and brachial plexus avulsion result in incomplete recovery of nerve function and permanent sensory loss [1,2]. Nerve *in situ* suturing is a common clinical approach to treating nerve injuries, with proven effectiveness in some cases [3]. However, conventional epineurium suturing techniques often fail in cases of peripheral nerve deficits with mismatched diameters or multiple distal nerves requiring simultaneous repair, due to issues such as high tension and suture failure. These limitations highlight the need for more advanced and adaptable nerve repair strategies.

Chitosan-based nerve conduits have gained attention as bioengineered scaffolds for peripheral nerve regeneration, owing to their biocompatibility, biodegradability, and tunable properties. Recently, a small gap sleeve-like biological suturing technique using chitosan conduits has been developed for peripheral nerve regeneration [4]. The approach eliminates the need for direct nerve stump suturing by employing a conical conduit, which bridges the gap between nerve stumps. The conical chitosan conduit can match the diameters of both proximal and distal nerves, avoiding the drawbacks of tension suturing and reducing the risk of suture failure [2,4]. While this technique has proven effective in single nerve displacement repairs, its application in repairing multiple distal nerves simultaneously remains unexplored. Furthermore, while the conduit prevents axonal misdirection and neuroma formation, it lacks intrinsic properties to actively promote axonal growth.

Vitamin B12, also known as cobalamin, is essential for the hematopoiesis and nervous tissue function [5,6]. Methylcobalamin (MeCbl), a methylated form of vitamin B12, serves as the essential cofactor for the transmethylation reaction that facilitates the conversion of homocysteine to methionine. Compared to other cobalamin analogues, including cyanocobalamin and hydroxylcobalamin, this form demonstrates superior binding affinity to nervous tissue [7]. Clinically, oral MeCbl has been effectively used in the

¹Department of Trauma and Orthopedics, Peking University People's Hospital, 100000 Beijing, China

²Key Laboratory of Trauma and Neural Regeneration, Peking University, 100000 Beijing, China

³Department of Physiology, School of Basic Medical Sciences, Shenzhen University, 518060 Shenzhen, Guangdong, China

⁴Department of Orthopedics, China-Japan Friendship Hospital, 100000 Beijing, China

⁵National Center for Trauma Medicine, 100000 Beijing, China

^{*}Correspondence: fengzhongxiaxi@163.com (Yusong Yuan); yuhuikou@bjmu.edu.cn (Yuhui Kou)

[†]These authors contributed equally. Academic Editor: Bettina Platt

management of various neuropathic conditions [8,9] and in slowing the progression of amyotrophic lateral sclerosis (ALS) [10]. From a mechistic perspective, MeCbl operated downstream of nerve growth factor and brain-derived neurotrophic factor, facilitating neuronal sprouting, regeneration, and enhanced neural conduction [7]. It has also been shown to have a particular affinity for nervous tissue, promoting myelination and nutrient transport [11]. These properties make MeCbl a promising candidate for promoting peripheral nerve transposition repair. However, the effects of different MeCbl dosages on Schwann cell function and the efficacy of nerve repair, especially in conjunction with chitosan conduits, require further investigation.

This investigation was designed to evaluate the efficacy of a novel repair strategy combining conical chitosan conduits and methylcobalamin administration for sciatic nerve transposition repair. We used a conical chitosan conduit to bridge the gap between the proximal common peroneal nerve and the distal tibial nerve and common peroneal nerve, facilitating small-gap nerve transposition. The biocompatibility of the conical chitosan conduit was assessed, and the effects of low-dose (50 µg/kg) and high-dose (200 μg/kg) MeCbl administration on nerve regeneration were evaluated in vivo. Functional outcomes were measured at 16 weeks post-surgery using gait analysis, electrophysiology, gastrocnemius muscle wet weight ratio, and nerve and muscle slices. This research elucidates the combined impact of conical chitosan conduits and MeCbl, offering a foundation for advancing peripheral nerve repair techniques in clinical settings.

2. Materials and Methods

2.1 Ethical Statement

All animal-related treatments were carried out in compliance with the Ethical Review Guidelines for Experimental Animals Welfare, approved by the Ethics Committee and Experimental Animal Center of Peking University People's Hospital in Beijing, China. The study followed the internationally recognized standards outlined in the Guide for the Care and Use of Laboratory Animals (NIH Publication No. 85-23, revised 1985). Animal welfare and experimental protocols were strictly maintained throughout the research period. Comprehensive documentation of animal-related data was prepared following the Animal Research: Reporting of In Vivo Experiments (ARRIVE) 2.0 guidelines [12].

2.2 Cell Culture

The rat Schwann cell line (RSC96) was sourced from the Shanghai Cell Bank of Chinese Academy of Sciences (GNR 6, Shanghai, China). The cell line was validated by PCR and tested negative for mycoplasma. The RSC96 cells exhibit two distinct morphologies: neuron-like and round cells. When the cells reach over-confluence, they tend to adopt a round morphology and become loosely adherent. Additionally, RSC96 cells are negative for surface recep-

tors such as nerve growth factor receptor (NGFR), platelet-derived growth factor receptor alpha (PDGFR α), and platelet-derived growth factor receptor beta (PDGFR β). After resuscitation, the cells were seeded into T25 flask (430639, Corning, NY, USA) and cultured for 24 h at 37 °C in a CO₂ incubator (Steri-Cycle 371, ThermoFisher Scientific, Waltham, MA, USA). Cells density was observed daily by inverted light microscope (ECLIPSE Ts2-FL, Nikon, Tokyo, Japan). When cells reached about 80% confluence, the cells were subcultured *via* digestion with 0.25% trypsin (25200056, Gibco, Green Island, NY, USA).

2.3 Fabrication of Conical Chitosan Conduit

The stainless steel mold used for fabricating the conical chitosan conduit is comprised of two cylindrical guiding rods with different diameters, linked together by a conical component. The diameter of thinner guiding rod measures 1.0 mm, whereas the thicker section has a diameter of 1.8 mm. The diameter of the guiding rod plays a critical role in the formation of the nerve conduit, as it directly influences how well it aligns with both the proximal common peroneal nerve and distal common peroneal and tibial nerves.

The conical chitosan conduit fabrication has been described in previous study [4] (Fig. 1). Chitosan powder (C915936, Macklin, Shanghai, China) with a degree of deacetylation greater than 70% was dissolved in 2% acetic acid solution (Beijing Chemical Factory, Beijing, China) to prepare 4% chitosan solution. At the same time, gelatin (G274269, Aladdin, Shanghai, China) was dissolved in warm water to form 1.6% gelatin solution. After mixing the two solutions, bubbles are removed using ultrasonication. The conical mold was immersed in the mixed chitosan solution. The mold surface was uniformly coated with chitosan solution, followed by solidification using 5% NaOH solution (S291866, Aladdin, Shanghai, China). The solidified chitosan was washed with deionized water for three times and dehydrated with acetone (Beijing Chemical Factory) for 2 min, dried at room temperature and placed in deacetylation solution (methanol: acetic anhydride = 1:1) for 10 minutes. Subsequently, the chitosan conduit was carefully detached from the mold to obtain hollow tubes with different inner diameters at both ends. Finally, the chitosan conduit was preserved in 75% ethanol for further animal experiments.

2.4 Biocompatibility Evaluation of Conical Chitosan Conduit

The biocompatibility of conical chitosan conduit was evaluated by live-dead staining and cell counting kit-8 (CCK-8) kits (CK04, Dojindo, Kumamoto, Japan). Briefly, the conical chitosan conduit was immersed in high-sugar complete medium at 37 °C for 72 h. Afterwards, Schwann cells in 24-well plate and 96-well plate were cultured in the extract (conical chitosan conduit soaking liquid) and fresh medium for 24 h and 72 h. Following the protocol



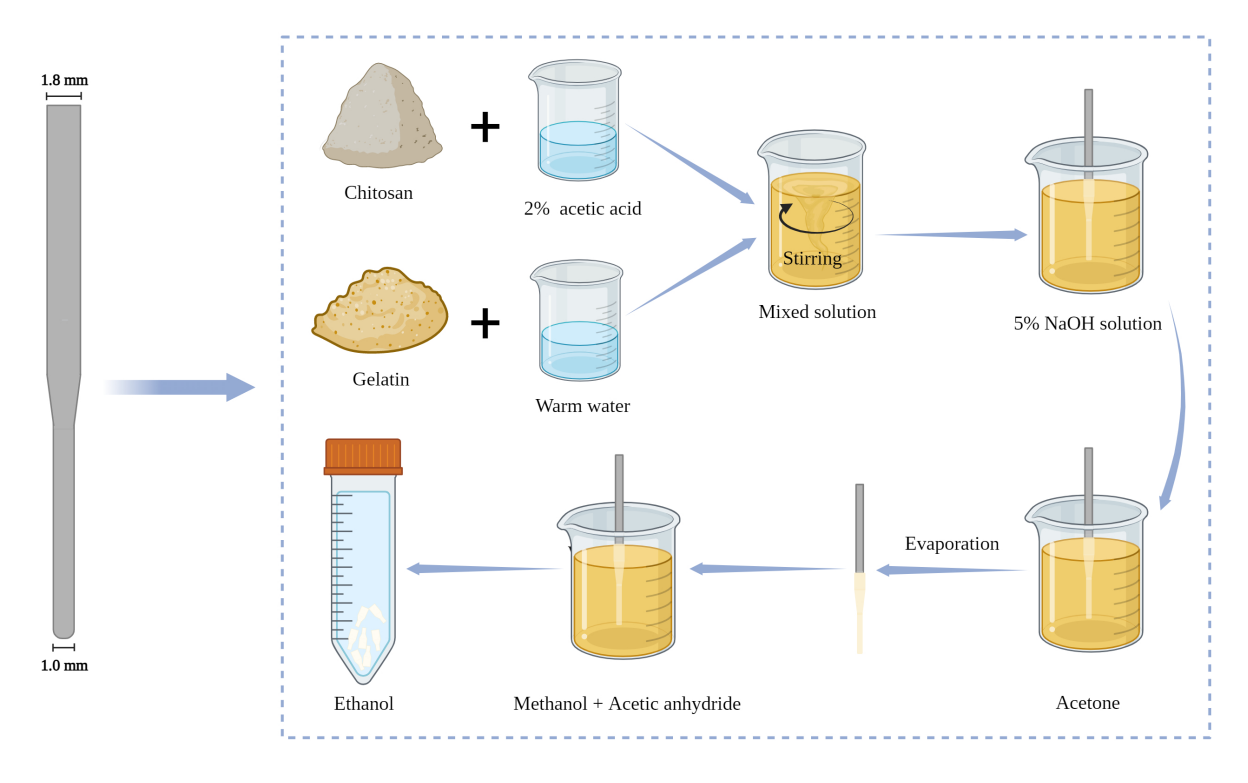


Fig. 1. Preparation process of conical chitosan conduit. Preparation mold on the left. This Figure was created with Biorender (https://www.biorender.com).

provieded with the live-dead staining kit (C2015S, Beyotime, Shanghai, China), Calcein-AM (green fluorescence) and propidium iodide (PI, red fluorescence) were used to stain Schwann cells. The cells were incubated at CO_2 incubator for 30 min, and observed with fluorescence microscope (ECLIPSE Ts2-FL, Nikon, Tokyo, Japan). In addition, the medium was removed from the 96-well plate after 24 h and 72 h, washed once with PBS, and 110 μ L mixed medium (Dulbecco's Modified Eagle's Medium (DMEM) medium 10:1 CCK-8 reagent) was added to each well. The cells were placed in the incubator for one hour, and the optical density (OD) value of each well was measured by microplate reader (iMark, BioRad, Hercules, CA, USA).

2.5 Animal Experiments

Female Sprague-Dawley (SD) rats (6 weeks, 200–230 g) were sourced from Beijing Vital River Laboratory Animal Technology (Beijing, China). These animals were housed in a controlled environment featuring a 12-hour cycle of light and darkness, with humidity levels maintained at 40%.

A total of 24 animals were randomly divided into four groups (n = 6 per group) (Fig. 2): sham group, chitosan conduit + normal saline group (Chi/NS), chitosan conduit +50 μ g/kg MeCbl group (Chi/50 μ g/kg), chitosan conduit +200 μ g/kg MeCbl group (Chi/200 μ g/kg). As previously described [13], rats in each group were anesthetized by inhalation of 2.5% isoflurane (R510-22-10, RWD, Shenzhen,

China), and then the skin of the right hind limb of rats was cleaned and disinfected before surgery. After that, the muscle gap was bluntly dissected, and the right common peroneal nerve and tibial nerve were exposed and transected at the 5 mm below the sciatic nerve fork. The proximal common peroneal nerve and distal common peroneal nerve and tibial nerve were bridged with the conical chitosan conduit using nylon suture with small gap of 2 mm. The proximal tibial nerve was sutured on the adjacent muscle in reverse direction to avoid self-repair. In the sham group, the muscle was carefully separated, allowing for the exposure of sciatic nerve and its branches, all while ensuring there was no damage to the nerve. After the surgery, sterile saline solution was administered daily throuth oral gavage to each rat in the sham and Chi/NS groups. In the meantime, each rat in the Chi/50 μg/kg and Chi/200 μg/kg group received oral treatment with methylcobalamin solution (HY-B0586, MedChemExpress LLC, Monmouth Junction, NJ, USA).

2.6 Postoperative Conditions of Rats

Rat were fed regularly and their daily progress was carefully recorded after surgery, including food consumption, body movements, recovery of surgical incisions, and movements of surgical limbs. Sixteen weeks post-surgery, an examination was conducted on the exposed common peroneal nerve and tibial nerve to determine if adhesions existed between the nerve structures and the adjacent tissues.



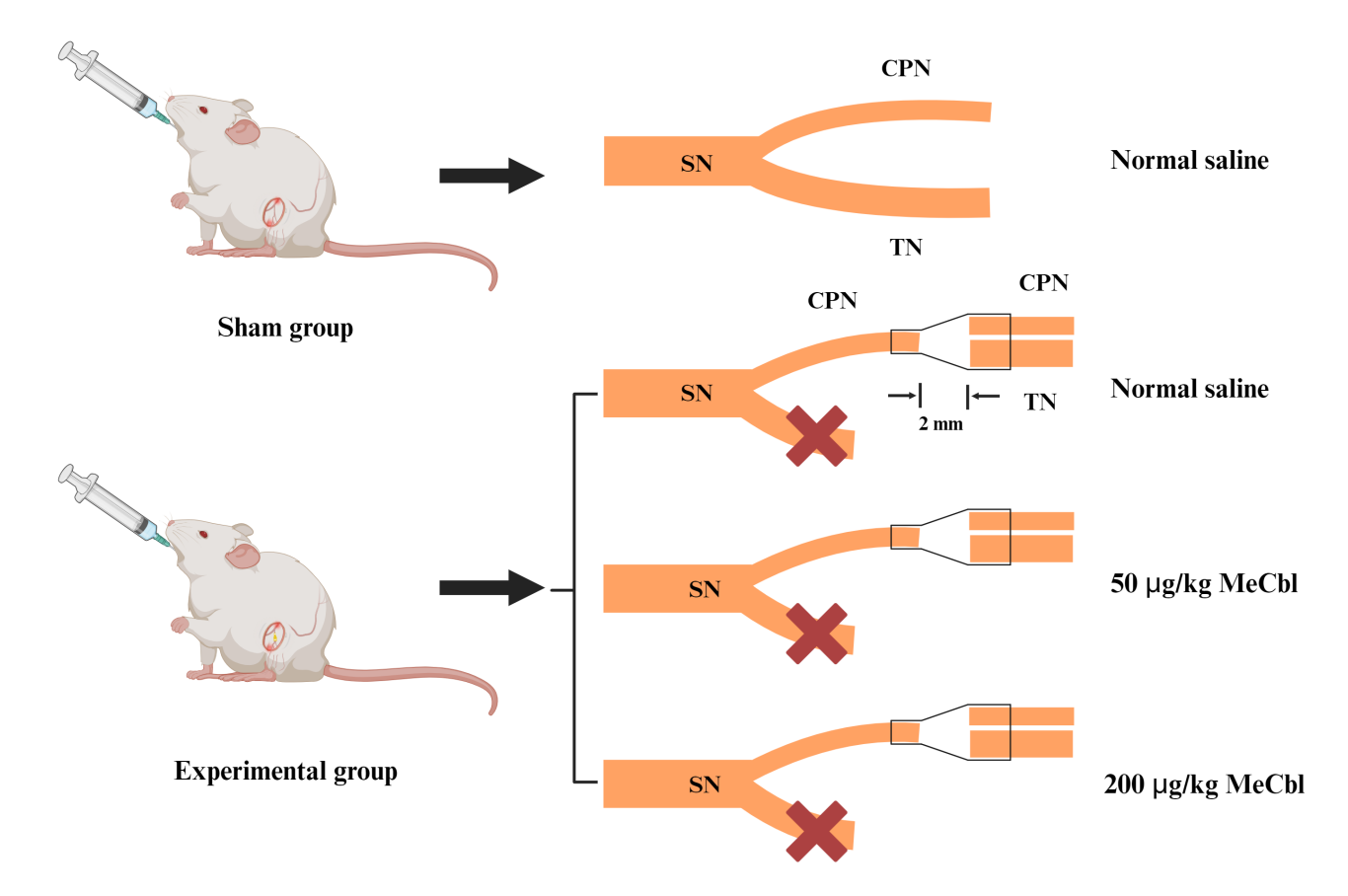


Fig. 2. Schematic illustration of animal model in this study. The sciatic nerve (SN) has two branches, including common peroneal nerve (CPN) and tibial nerve (TN). In the experimental group, the CPN and TN were cut 5 mm away from the point where they split into two branches. A conical chitosan conduit was used to bridge the proximal CPN with the distal CPN and TN. This Figure was created with Biorender (https://www.biorender.com). MeCbl, methylcobalamin.

2.7 Gait Analysis

Gait analysis was conducted 16 weeks post-surgery. Gait analysis system (ZS-BT/S, Zhongshi Dichuang Technology, Beijing, China) recorded and evaluated the rats' footprints. Prior to the experiment, all rats were acclimated to the testing environment. Subsequently, each rat passed through a closed runway consisting of a bottom glass plate and a partition. Footprints from each rat were aptured using a high-speed camera. The sciatic function index (SFI) for each animal was determined using the following formula [13]:

$$SFI = \frac{109.5 \; (ETS-NTS)}{NTS} - \frac{38.3 \; (EPL-NPL)}{NPL} + \frac{13.3 \; (EITS-NITS)}{NITS} - 8.8$$

In this formula, exprimental print length (EPL) denotes the measurement taken from the heel to the apex of the third toe, while normal print length (NPL) indicates the standard length from heel to third toe. Experimental toe spread (ETS) signifies the experimental distance measured from the first to the fifth toe, with normal toe spread (NTS) representing the typical length from the first to the fifth toe. Experimental inter toe spread (EITS) refers to the experimental measurement stretching from the second to the

fourth toe, and normal inter toe spread (NITS) is the normal length between the second and fourth toes. An SFI score of 0 indicates normal motor function, and a score of -100 suggests complete impairment of motor function.

2.8 Electrophysiological Analysis

Rats were anesthetized by inhaling 2.5% isoflurane (R510-22-10, RWD) at 16 weeks after surgery. We used electrophysiological instruments (Oxford Instruments, Oxford, UK) to record the amplitude and latency of compound motor action potential (CMAP). The stimulating electrode was positioned at distal tibial nerve, and the recording electrodes were inserted into the proximal and distal sides of the gastrocnemius. Then, the amplitude and latency of CMAP in each group were induced by rectangular pulse.

2.9 Immunofluorescence Staining

Rats were euthanized throuth carbon dioxide inhalation with a filling rate of 30%–70% per minute, and a segment measuring the distal 5 mm of the tibial nerve conduit was obtained. The distal tibial nerve was fixed using 4% paraformaldehyde (P1110, Solarbio, Beijing, China) and dehydrated in a 30% sucrose solution. Subsequently, the



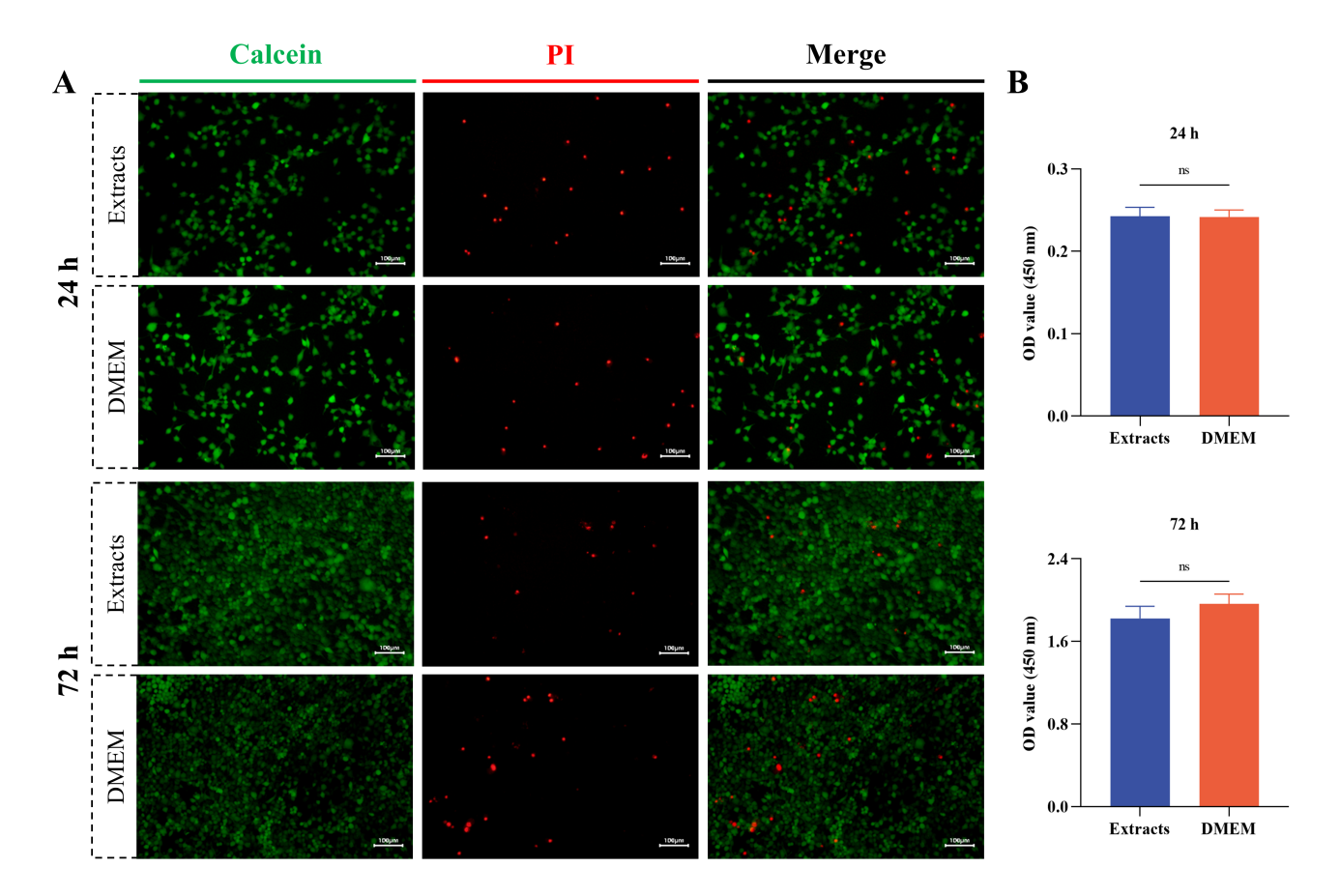


Fig. 3. Biocompatibility evaluation of conical chitosan conduit. (A) The live rat Schwann cell line (RSC96) was labeled with Calcein (green). The dead RSC96 cells were labeled with propidium iodide (PI, red). Scale bar = $100 \mu m$. (B) Cell counting kit-8 (CCK-8) assay for RSC96 cells treated with extracts and Dulbecco's Modified Eagle's Medium (DMEM) at 24 h and 72 h. n = 3 per group. ns, no significance; OD, optical density.



Fig. 4. Conical chitosan conduit and nerve transposition repair. (A) Representative image of conical chitosan conduit with different inner diameters. (B) Conical chitosan conduit during transposition repair model surgery. The white arrow indicated the proximal common peroneal nerve. (C) The proximal common peroneal nerve connected the distal common peroneal nerve and tibial nerve at 16 weeks after surgery. The white arrow indicated distal common peroneal nerve (up), and distal tibial nerve (down).

tissue was sliced into transverse sections of 10 μ m thickness utilizing a freezing microtome (CM1950 OUVV, Leica, Wetzlar, Germany). In each group, the nerve tissue sections were incubated overnight at 4 °C with primary antibodies NF200 (1:400, N4142, MilliporeSigma, Burlington, MA, USA) and S100 (1:400, S2532, MilliporeSigma).

After being washed three times with PBS, the sections underwent incubation for 1 h at room temperature with a mixture of secondary antibodies: Alexa488 (1:500, ab150077, Abcam) and Alexa594 (1:500, ab150116, Abcam, Cambridge, UK). Finally, the sections were sealed with quench-proof tablet containing DAPI (P0131, Beyotime) and ob-



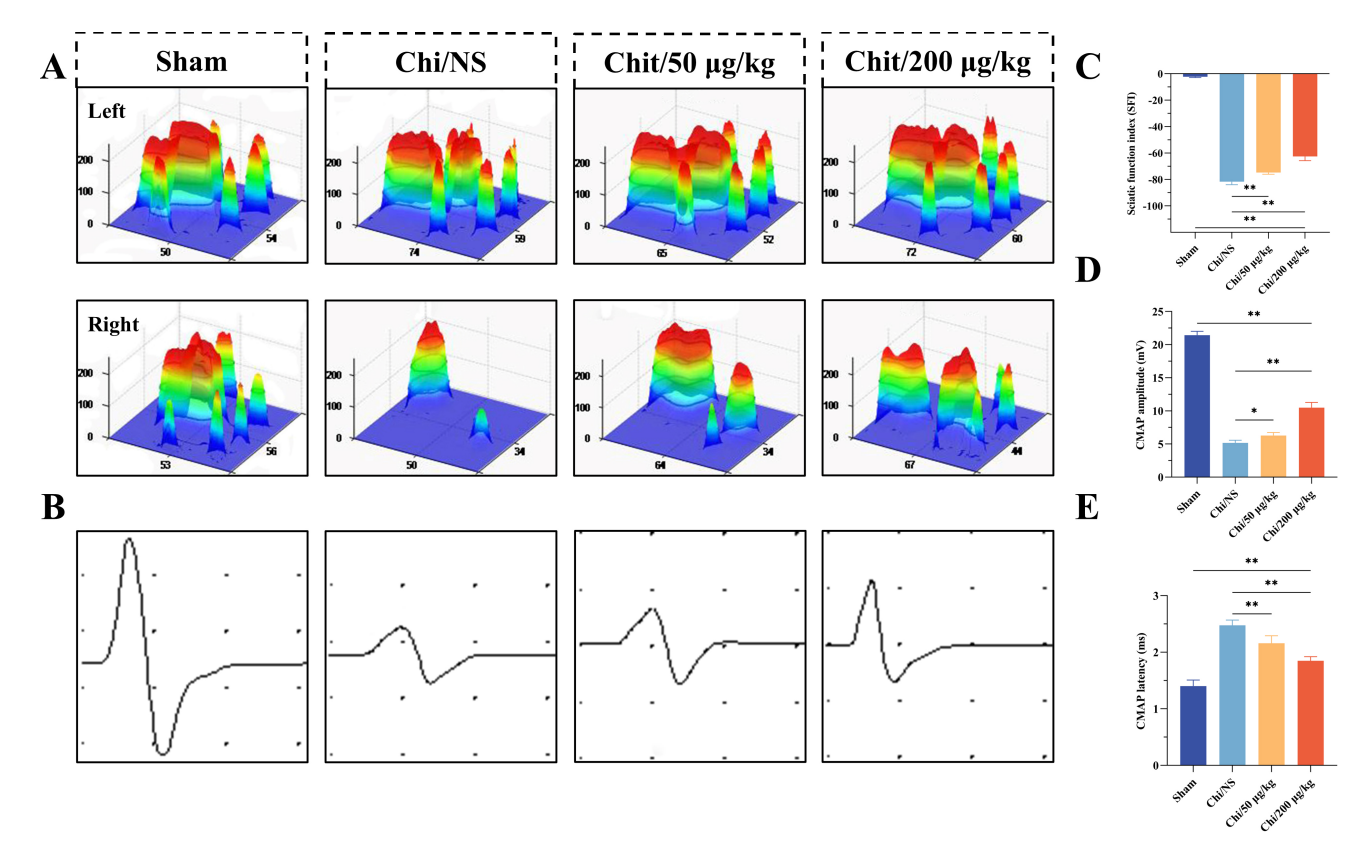


Fig. 5. Evaluation of motor function and nerve conduction function. (A) Typical 3D stress distribution patterns for each group at 16 weeks post-surgery. (B) Characteristic electrophysiological recordings of compound muscle action potentials (CMAPs) from different groups. Horizontal axis: ms, Vertical axis: mV. (C) The sciatic nerve function index (SFI) in each group. (D) CMAP amplitude measurements for each group. (E) CMAP latency measurements for each group. n = 6 per group. *p < 0.05, **p < 0.01. Chit, chitosan; Chi/NS, chitosan conduit+normal saline.

served at $100 \times$ magnification using fluorescence microscope (ECLIPSE Ts2-FL, Nikon).

2.10 Morphological Analysis of Axonal Regeneration

The regenerated tibial nerve was collected from the distal ends of conical chitosan conduit at 16 weeks postsurgery. The nerve specimens were preserved in 2.5% glutaraldehyde (P1126, Solarbio) for 24 h at 4 °C, followed by staining with 1% osmium tetroxide (251755, Sigma-Aldrich, Taufkirchen, Germany) and dehydrated using gradient concentrations of acetone. The nerve tissue was then embedded in epoxy resin, sliced into semithin transverse sections measuring 700 nm in thichness and ultrathin transverse sections that were 70 nm thick. The semithin sections underwent staining with 1% toluidine blue (G3663, Solarbio) to assess density of myelinated nerve fibers at $200\times$ magnification, while the ultrathin sections were stained with uranyl acetate and leas citrate to evaluate myelin thickness and diameters of myelinated axons through transmission electron microscopy (TEM, JEM-1400, JEOL, Tokyo, Japan). The images were analyzed with Fiji Image J software (National Institutes of Health, Bethesda, MD, USA).

2.11 Wet Weight Ratio and Histological Analysis of Gastrocnemius

At 16 weeks post-implantation of a nerve conduit, the right gastrocnemius from the implanted limb and the corresponding muscles from the left limb were harvested and immediately weighed with electronic balance (Sartorius, Beijing, China). The ratio of wet weight (right to left) was calculated. Muscle samples were preserved in GD fixative solution (G1111, Servicebio, Wuhan, Hubei, China) for 48 h at 4 °C, followed by dehydration using 15% and 30% sucrose solution. Subsequently, the gastrocnemius muscle was embedded in paraffin and sliced transversely into sections with a thickness of 10 µm. These sections were then stained using the Masson's trichrome staining kit (G1340, Solarbio) to visualize muscle fibers. For quantitative analysis, five random fields from each section were chosen, and the cross-sectional area of the muscle fibers was measured using Fiji Image J software.

2.12 Statistical Analysis

The results are expressed as the mean \pm SD. Statistical analysis was performed with Graphpad Prism 8.0 (Graph-Pad Software, CA, USA). Intergroup comparisons were as-



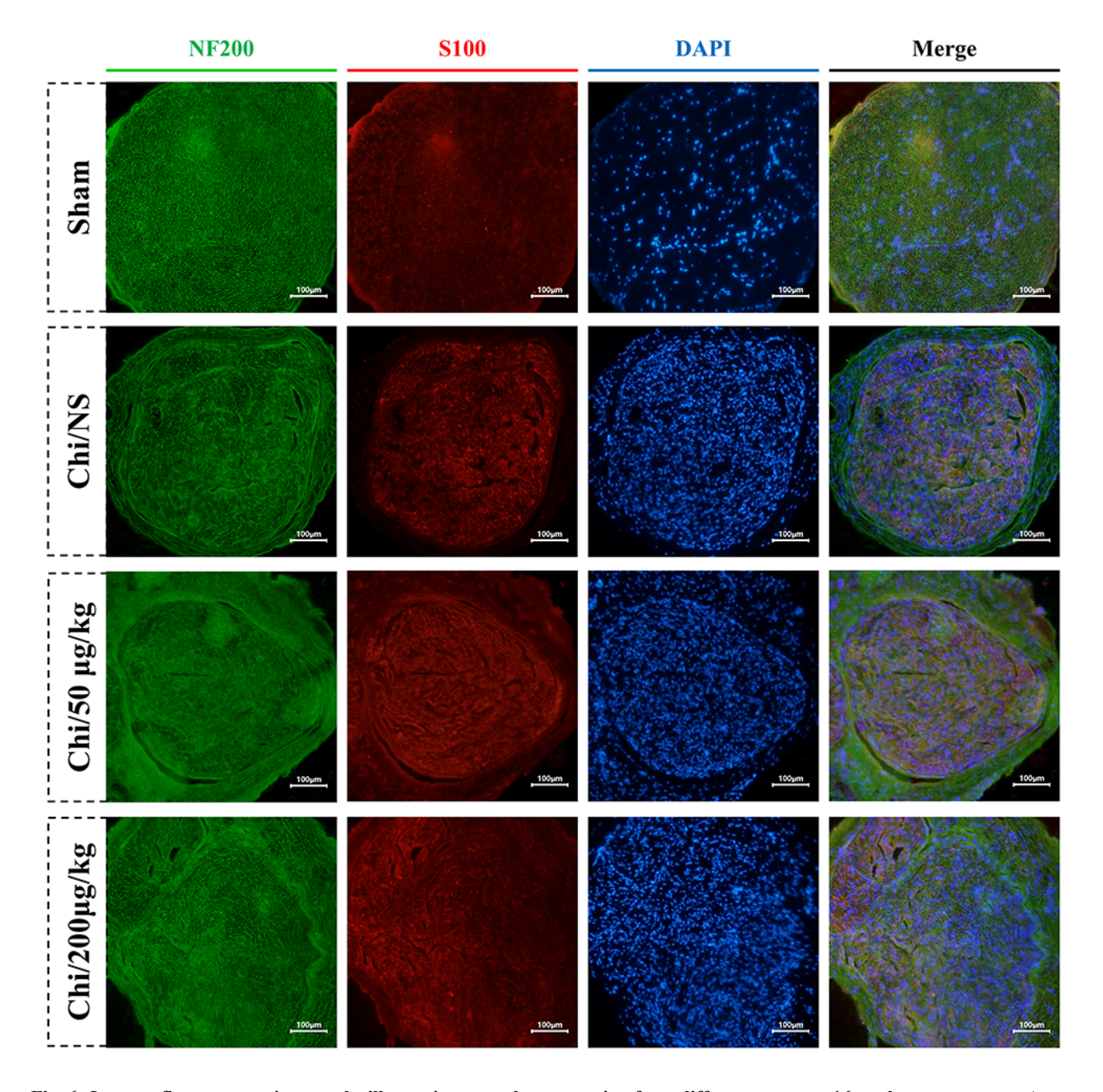


Fig. 6. Immunoflurescence micrographs illustrating axonal regeneration from different group at 16 weeks post-surgery. Axons are identified by green fluorescence (NF200), while Schwann cells are marked with red fluorescence (S100). The nuclei are highlighted using blue fluorescence (DAPI). Scale bar = $100 \ \mu m$.

sessed by t-test, while multigroup comparisons were analyzed through one-way ANOVA followed by Tukey's post hoc test. Statistical significance was defined as p value < 0.05.

3. Results

3.1 Conical Chitosan Conduit With Favorable Biocompatibility

As shown in Fig. 3, the results of live-dead staining and CCK-8 assay demonstrated that the conical chitosan conduit possessed good biocompatibility. After 24 h and

72 h of treatment with the extracts and complete DMEM medium, the live RSC96 cells were labeled green with Calcein, while PI staining labeled dead cells as red (Fig. 3A). The quantitative analysis of CCK-8 assay further demonstrated that the extracts from conical chitosan conduit had no effect on RSC96 cell viability at 24 h and 72 h compared to DMEM group (p > 0.05, Fig. 3B).

3.2 General Observation

Fig. 4A illustrated that the chitosan conduit is transparent. The inner diameters at each end of the conduit dif-



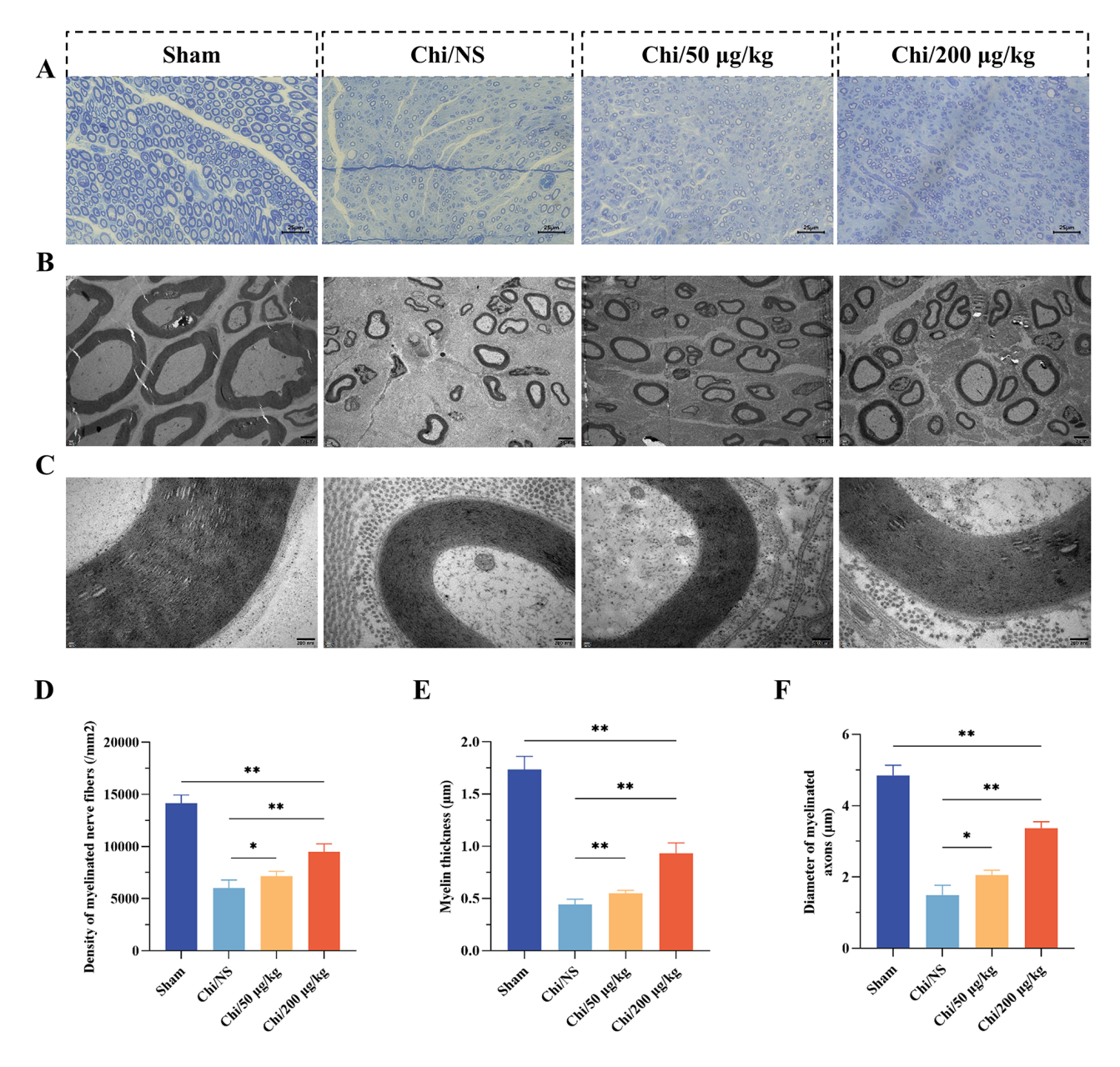


Fig. 7. Histological assessment of nerve regeneration. (A) Representative micrograph depicting toluidine-blue staining for each group. Scale bar = 25 μ m. (B) Exemplary TEM image corresponding to each group. Scale bar = 2 μ m. (C) Enlarged view of the micrograph depicted in (B). Scale bar = 200 nm. (D) Density of myelinated nerve fibers in each group. (E) Thickness measurement of myelinated axons within each group. (F) Determination of myelinated axons diameter across each group. n = 6 per group. n = 6 per group. n = 6 per group.

fer, with the narrower end measuring 1.0 mm and the wider end measuring 1.8 mm. A conical structure bridges the two ends. Fig. 4B showed that the diameter of the nerves corresponds to the inner diameter of the conduit. As shown in Fig. 4C, by the 16-week post-surgery mark, the conduit underwent partial absorption, and no noticeable signs of inflammation or neuroma were observed at the nerve suture site.

3.3 Recovery of Motor Function and Electrophysiology

SFI serves as an objective indicator for assessing motor function recovery in rat model. The 3D footprints pat-

terns presented in Fig. 5A demonstrated comparable morphology between left and right footprints in the sham group. Statistical analysis of SFI data (Fig. 5C) revealed significant improvement in both Chi/50 µg/kg and Chi/200 µg/kg groups compared to the Chi/NS group (p < 0.01). However, the Chi/200 µg/kg group showed inferior performance relative to the sham group at the 16 weeks (p < 0.01).

Electrophysiological assessments were performed to evaluate the recovery of nerve conductivity on surgical side (Fig. 5B). The CAMP amplitude in the tibial nerve serves as an indicator of the quantity of innervated gastrocnemius fibers, while the CAMP latency correlates with the degree



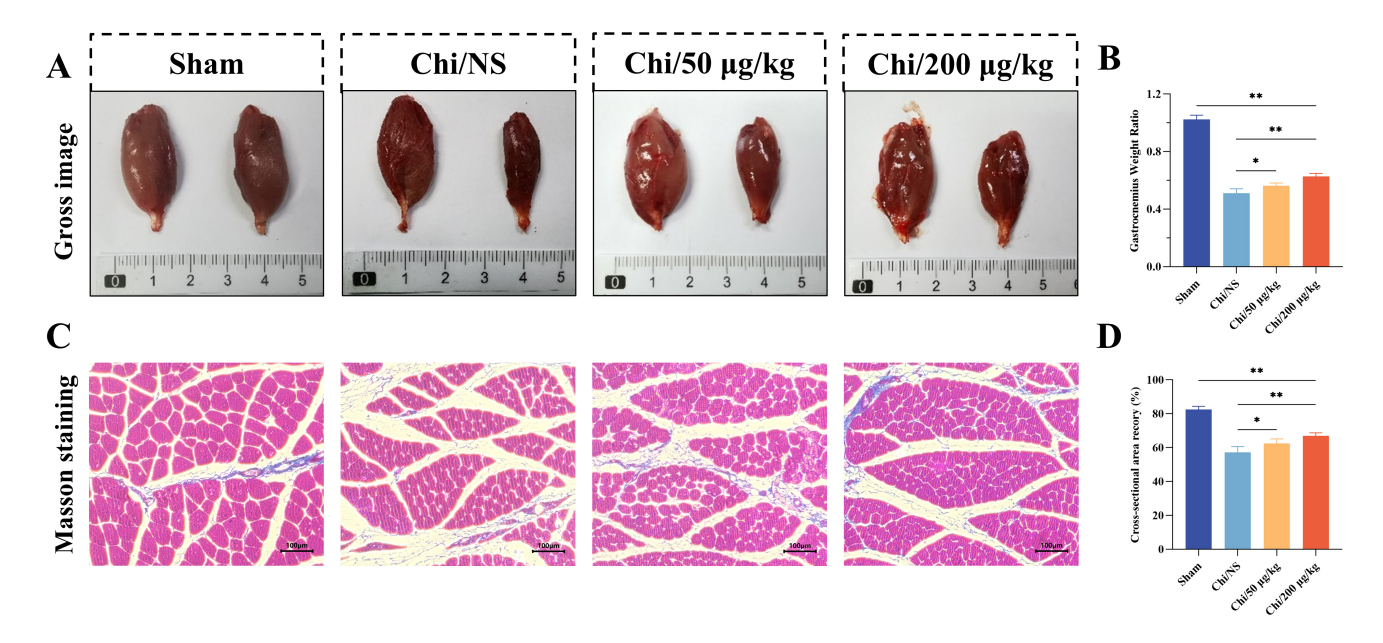


Fig. 8. Histological evaluation of the gastrocnemius. (A) Comparative image showing healthy (left) and injured (right) gastrocnemius muscles. (B) Ratio of wet weights of injured to healthy muscles across groups. (C) Masson's trichrome staining in transverse sections of the right gastrocnemius. Scale bar = 100 μ m. (D) Cross-sectional area recovery index of muscle (%) in each group. n = 6 per group. p = 0.05, p = 0.01.

of myelination in regenerated axons. The CAMP amplitude of the right hindlimb in the Chi/NS group was lower compared to the Chi/50 μ g/kg and Chi/200 μ g/kg group (p < 0.05, Fig. 5D), which indicated the methylcobalamin administration improved muscle innervation, and was more effective at high concentration (200 μ g/kg). Corresponding to the above results, the CMAP latency was obviously higher in the Chi/NS group without MeCbl treatment (p < 0.01, Fig. 5E).

3.4 Immunofluorescence and Histological Evaluation of Regenerated Axons and Myelin

Double NF200/S100 immunofluorescence staining of distal tibial nerve in each group was performed at 16 weeks. As shown in Fig. 6, immunofluorescence analysis demonstrated distinct labeling patterns, with NF200-positive regenerated axons exhibiting green fluorescence and S100-positive Schwann cells displaying red fluorescence. The staining images indicated that more axonal regeneration and myelination in both Chi/50 $\mu g/kg$ and Chi/200 $\mu g/kg$ groups compared to the Chi/NS group.

The results of TEM analysis and toluidine blue staining on nerve cross-sections were presented in Fig. 7. Fig. 7A presented toluiding blue-stained images for each group, with myelinated fiber density quantified in Fig. 7D. Quantitative analysis revealed a significant reduction in myelinated fiber density per unit area in the Chi/NS group compared to both Chi/50 μ g/kg (p < 0.05) and Chi/200 μ g/kg (p < 0.01) groups. Ultrastructural examination through TEM (Fig. 7B,C) showed enhanced myelin thickness in regenerated tibial nerve fibers from Chi/50 μ g/kg

and Chi/200 µg/kg groups versus Chi/NS group (p < 0.01, Fig. 7E), indicating MeCbl-mediated Schwann cell myelination promotion. Furthermore, myelinated axon diameters in Chi/NS group were smaller than those in Chi/50 µg/kg (p < 0.05) and Chi/200 µg/kg (p < 0.01) groups (Fig. 7F).

3.5 Gastrocnemius Muscle Recovery

Denervated muscles undergo varying degrees of atrophy due to loss of contraction. Gastrocnemius muscles from both hindlimbs were dissected and weighed at 16 weeks post-surgery. Fig. 8A showed typical images of operated and contralateral gastrocnemius muscles in each group. The gastrocnemius wet weight ratio (right/left) was higher in the Chi/50 μ g/kg (p < 0.05) and Chi/200 μ g/kg (p < 0.01) groups compared to the Chi/NS group, but lower than the sham group (p < 0.01, Fig. 8B). Moreover, the transverse sections of operated gastrocnemius muscle were stained with Masson's trichrome, and Fig. 8C showed the representative images of Masson's trichrome staining of gastrocnemius muscle fibers. Using Masson's trichrome staining, we noticed a notable reduction in the presence of vacant areas between muscle fibers were observed in the sham and Chi/200 µg/kg groups. The muscle fiber cross-sectional area recovery (%) of the Chi/NS group showed a reduction compared to the Chi/50 μ g/kg (p < 0.05) and Chi/200 μ g/kg groups (p < 0.01) (Fig. 8D).

4. Discussion

Peripheral nerve transposition repair has been extensively studied in both clinical and animal research. For



instance, nerve transposition techniques, such as those involving the musculocutaneous nerve, medial pectoral nerve, radial nerve's muscular branches, and anterior interosseous in relation to ulnar nerve repair [2]. Additionally, brachial plexus injuries can be treated through the transposition of cervical spinal nerve 7 (either ipsilateral or contralateral), accessory nerve, and phrenic nerve [4]. In this study, we aimed to address the challenge of simultaneous repair and promotion of nerve regeneration in multiple distal nerves following peripheral nerve injury. We used conical chitosan conduits to bridge a 2 mm defect between the proximal common peroneal and distal common peroneal and tibial nerves in rats.

Chitosan is widely prepared into hydrogel [14], wound dressing [15], and nerve conduits [16] due to its favorable antibacterial, biocompatible, and degradable property in regenerative medicine. In this study, RSC96 cells survived well in the extract solution of conical chitosan conduit detected by live-dead staining and CCK-8 assay, indicating that the nerve conduit is biocompatible and suitable for nerve regeneration applications. Compared to the traditional epineurial suture and silicone conduits, chitosan conduit has the following advantages: (1) The proximal and distal ends of nerve can be sutured without tension. (2) The gap between the stump of the nerve is very small. This gap will not affect nerve regeneration and improve the accuracy of nerve regeneration selection. (3) The good biodegradability and flexibility allow the conduit not to compress the regenerated axons and remove the conduit after second operation, resulting in nerve injury again. However, it is important to note that chitosan conduits may induce mild inflammatory responses in vivo and can be encapsulated by fibrous tissue as a foreign body. Additionally, the degradation of chitosan conduits can be somewhat unstable, and the degradation period varies depending on the molecular weight of the chitosan and the degree of acetylation. Moreover, the application of conical chitosan conduit in transposition repair of rat peripheral nerve is not limited to single donor-to-receptor nerve repair models, but can also be extended to simultaneous repair of multiple using a single donor nerve.

Numerous studies have demonstrated that MeCbl exhibited nerve regeneration-promoting effects in both clinical and basic applications [17–19]. In case of sciatic nerve crush injury, early co-administration of MeCbl (500 µg/kg) and vitamin E acetate was found to significantly improve paw withdrawal latency, accompanied by reduction of thermal hyperlagesia and increase of motor nerve conduction velocity [20]. Similarly, we evaluated the therapeutic effectiveness of MeCbl at various concentrations. Our findings demonstrated that the conical chitosan conduit combined with MeCbl effectively bridged multiple distal nerves and promoted nerve regeneration. To explore the mechanism of MeCbl neuroprotection, Okada *et al.* [21] found that MeCbl increased the activity of ERK1/2 and Akt through

the methylation cycle for nerve regeneration *in vitro*. Moreover, the local application of MeCbl can avoid metabolic clearance. Zhang *et al.* [22] transplanted MeCbl-loaded nerve conduits into rats and induced regeneration of 10 mm sciatic nerve defects, and achieved sustained release of MeCbl up to 21 days.

In current research, the evaluation of motor function recovery using the SFI revealed significant improvement in the Chi/50 µg/kg and Chi/200 µg/kg groups compared to the Chi/NS group. The SFI results indicated enhanced motor function recovery in the treated groups, suggesting that the conical chitosan conduit combined with MeCbl administration facilitated functional restoration after peripheral nerve injury. Electrophysiological assessment of nerve conduction demonstrated that MeCbl administration improved muscle innervation, as reflected by increased CMAP amplitudes. The higher concentration of MeCbl (200 μg/kg) resulted in superior outcomes, indicating a dose-dependent effect. Furthermore, the CMAP latency was significantly lower in the Chi/50 µg/kg and Chi/200 µg/kg groups compared to the Chi/NS group, suggesting improved myelin thickness of regenerated axons. These results indicate that MeCbl promotes nerve conduction and enhances myelination of Schwann cells, ultimately contributing to functional recovery. TEM images supported these findings, showing increased myelin thickness and axon diameter in the Chi/50 µg/kg and Chi/200 μg/kg groups. These results suggest that MeCbl administration in conjunction with the conical chitosan conduit enhances axon regeneration and myelination, which are crucial for functional recovery. The dose-dependent effects observed suggest that higher concentrations of MeCbl may yield more favorable outcomes. The optimal concentration and duration of MeCbl administration should be further explored to establish the most effective treatment regimen. Additionally, long-term follow-up studies are necessary to assess the durability of the nerve regeneration and functional recovery achieved using the conical chitosan conduit and MeCbl combination.

There are other similar strategies used to speed up peripheral nerve regeneration. Based on the small gap suture technique, the nerve regeneration chamber microenvironment was constructed through nerve conduit to achieve early vascular regeneration, effective nerve growth, and continuous nutritional support. Yang et al. [23] loaded exosomes derived from adipose-derived stem cells (ADSCs) into nerve guidance conduits containing alginate hydrogel, which released the exosomes in a continuous and stable way, and successfully repaired the 10 mm sciatic nerve defect in rats. Furthermore, bioactive peptide-loaded aligned chitosan nanofiber hydrogel showed a positive effect on peripheral nerve regeneration [24]. However, these animal models are only a single nerve defect, and the application of these bioactive materials in peripheral nerve transposition repair still needs to be further explored.



5. Conclusions

To sum up, our study demonstrates that the application of conical chitosan conduit combined with MeCbl effectively bridges multiple distal nerves. This approach enhances both nerve regeneration and functional recovery after peripheral nerve injuries. The favorable biocompatibility of the chitosan conduit and the therapeutic effectiveness of MeCbl on motor function, nerve conduction, axon regeneration, myelination, and muscle recovery highlight the potential clinical application of this approach. Further research is needed to optimize the treatment strategies and assess the long-term outcomes.

Availability of Data and Materials

The data are available from the corresponding author upon reasonable request.

Author Contributions

QCL, YSY, and YHK designed the study. QCL wrote the manuscript. QCL and FSZ performed the experiments.FSZ and SYL contributed to data analysis and interpreted data. YHK supervised the entire work and obtained funding support. YHK and YSY reviewed and revised the manuscript and gave final approval to publish this paper. All authors contributed to editorial changes in the manuscript. All authors read and approved the final manuscript. All authors have participated sufficiently in the work and agreed to be accountable for all aspects of the work.

Ethics Approval and Consent to Participate

The animal protocols and treatments were conducted in accordance with the Guidelines for Ethical Review of Experimental Animals for Animal Welfare, as approved by the Ethics Committee and Experimental Animal Center of Peking University People's Hospital in Beijing, China. The study received ethical approval under permit number 2022PHE050. All surgical procedures and animal care followed the standards set by the National Institutes of Health Guide for the Care and Use of Laboratory Animals (NIH Publication No. 85-23, revised 1985). Furthermore, all relevant information regarding the animals was reported in compliance with the ARRIVE 2.0 guidelines.

Acknowledgment

We are grateful for the assistance of Biorender (biorender.com) in the construction of some figures.

Funding

This work was supported by the National Natural Science Foundation of China [NO.32371048].

Conflict of Interest

The authors declare no conflict of interest.

References

- [1] Hsieh YL, Yang NP, Chen SF, Lu YL, Yang CC. Early Intervention of Cold-Water Swimming on Functional Recovery and Spinal Pain Modulation Following Brachial Plexus Avulsion in Rats. International Journal of Molecular Sciences. 2022; 23: 1178. https://doi.org/10.3390/ijms23031178.
- [2] Yu F, Yu YL, Niu SP, Zhang PX, Yin XF, Han N, et al. Repair of long segmental ulnar nerve defects in rats by several different kinds of nerve transposition. Neural Regeneration Research. 2019; 14: 692–698. https://doi.org/10.4103/1673-5374.247473.
- [3] Hopf A, Al-Bayati L, Schaefer DJ, Kalbermatten DF, Guzman R, Madduri S. Optimized Decellularization Protocol for Large Peripheral Nerve Segments: Towards Personalized Nerve Bioengineering. Bioengineering (Basel, Switzerland). 2022; 9: 412. https://doi.org/10.3390/bioengineering9090412.
- [4] Kou YH, Yu YL, Zhang YJ, Han N, Yin XF, Yuan YS, *et al.* Repair of peripheral nerve defects by nerve transposition using small gap bio-sleeve suture with different inner diameters at both ends. Neural Regeneration Research. 2019; 14: 706–712. https://doi.org/10.4103/1673-5374.247475.
- [5] Bellazzi F, Bertolaso M. Emergence in Complex Physiological Processes: The Case of Vitamin B12 Functions in Erythropoiesis. Systems. 2024; 12: 131. https://doi.org/10.3390/systems12040131.
- [6] Baltrusch S. The Role of Neurotropic B Vitamins in Nerve Regeneration. BioMed Research International. 2021; 2021: 9968228. https://doi.org/10.1155/2021/9968228.
- [7] Liao WC, Wang YJ, Huang MC, Tseng GF. Methylcobalamin facilitates collateral sprouting of donor axons and innervation of recipient muscle in end-to-side neurorrhaphy in rats. PloS One. 2013; 8: e76302. https://doi.org/10.1371/journal.pone.0076302.
- [8] Sharma C, Kaur I, Singh H, Grover IS, Singh J. A randomized comparative study of methylcobalamin, methylcobalamin plus pregabalin and methylcobalamin plus duloxetine in patients of painful diabetic neuropathy. Indian Journal of Pharmacology. 2021; 53: 358–363. https://doi.org/10.4103/ijp.ijp_1159_20.
- [9] Sawangjit R, Thongphui S, Chaichompu W, Phumart P. Efficacy and Safety of Mecobalamin on Peripheral Neuropathy: A Systematic Review and Meta-Analysis of Randomized Controlled Trials. Journal of Alternative and Complementary Medicine. 2020; 26: 1117–1129. https://doi.org/10.1089/acm.2020.0068.
- [10] Kaji R, Imai T, Iwasaki Y, Okamoto K, Nakagawa M, Ohashi Y, et al. Ultra-high-dose methylcobalamin in amyotrophic lateral sclerosis: a long-term phase II/III randomised controlled study. Journal of Neurology, Neurosurgery, and Psychiatry. 2019; 90: 451–457. https://doi.org/10.1136/jnnp-2018-319294.
- [11] Mizukami H, Ogasawara S, Yamagishi SI, Takahashi K, Yagihashi S. Methylcobalamin effects on diabetic neuropathy and nerve protein kinase C in rats. European Journal of Clinical Investigation. 2011; 41: 442–450. https://doi.org/10.1111/j.1365-2362.2010.02430.x.
- [12] Percie du Sert N, Hurst V, Ahluwalia A, Alam S, Avey MT, Baker M, *et al.* The ARRIVE guidelines 2.0: Updated guidelines for reporting animal research. PLoS Biology. 2020; 18: e3000410. https://doi.org/10.1371/journal.pbio.3000410.
- [13] Zhang F, Li Q, Ma B, Zhang M, Kou Y. Chitosan-Based Conduits with Different Inner Diameters at both Ends Combined with Modified Formula Radix Hedysari Promote Nerve Transposition Repair. Frontiers in Bioscience (Landmark Edition). 2023; 28: 298. https://doi.org/10.31083/j.fbl2811298.
- [14] Song F, Kong Y, Shao C, Cheng Y, Lu J, Tao Y, *et al.* Chitosan-based multifunctional flexible hemostatic bio-hydrogel. Acta Biomaterialia. 2021; 136: 170–183. https://doi.org/10.1016/j.actbio.2021.09.056.
- [15] Cao Y, Yin J, Shi Y, Cheng J, Fang Y, Huang C, et al. Starch



- and chitosan-based antibacterial dressing for infected wound treatment via self-activated NO release strategy. International Journal of Biological Macromolecules. 2022; 220: 1177–1187. https://doi.org/10.1016/j.ijbiomac.2022.08.152.
- [16] Zhang F, Wu X, Li Q, Ma B, Zhang M, Zhang W, et al. Dual growth factor methacrylic alginate microgels combined with chitosan-based conduits facilitate peripheral nerve repair. International Journal of Biological Macromolecules. 2024; 268: 131594. https://doi.org/10.1016/j.ijbiomac.2024.131594.
- [17] Suzuki K, Tanaka H, Ebara M, Uto K, Matsuoka H, Nishimoto S, et al. Electrospun nanofiber sheets incorporating methylcobal-amin promote nerve regeneration and functional recovery in a rat sciatic nerve crush injury model. Acta Biomaterialia. 2017; 53: 250–259. https://doi.org/10.1016/j.actbio.2017.02.004.
- [18] Hsieh YL, Lu YL, Yang NP, Yang CC. Methylcobalamin in Combination with Early Intervention of Low-Intensity Pulsed Ultrasound Potentiates Nerve Regeneration and Functional Recovery in a Rat Brachial Plexus Injury Model. International Journal of Molecular Sciences. 2023; 24: 13856. https://doi.org/10. 3390/ijms241813856.
- [19] Shibuya K, Misawa S, Nasu S, Sekiguchi Y, Beppu M, Iwai Y, et al. Safety and efficacy of intravenous ultra-high dose methyl-cobalamin treatment for peripheral neuropathy: a phase I/II open label clinical trial. Internal Medicine. 2014; 53: 1927–1931. https://doi.org/10.2169/internalmedicine.53.1951.
- [20] Morani AS, Bodhankar SL. Early co-administration of vitamin

- E acetate and methylcobalamin improves thermal hyperalgesia and motor nerve conduction velocity following sciatic nerve crush injury in rats. Pharmacological Reports. 2010; 62: 405–409. https://doi.org/10.1016/s1734-1140(10)70281-4.
- [21] Okada K, Tanaka H, Temporin K, Okamoto M, Kuroda Y, Moritomo H, et al. Methylcobalamin increases Erk1/2 and Akt activities through the methylation cycle and promotes nerve regeneration in a rat sciatic nerve injury model. Experimental Neurology. 2010; 222: 191–203. https://doi.org/10.1016/j.expneurol.2009. 12.017.
- [22] Zhang D, Yang W, Wang C, Zheng H, Liu Z, Chen Z, et al. Methylcobalamin-Loaded PLCL Conduits Facilitate the Peripheral Nerve Regeneration. Macromolecular Bioscience. 2020; 20: e1900382. https://doi.org/10.1002/mabi.201900382.
- [23] Yang Z, Yang Y, Xu Y, Jiang W, Shao Y, Xing J, *et al.* Biomimetic nerve guidance conduit containing engineered exosomes of adipose-derived stem cells promotes peripheral nerve regeneration. Stem Cell Research & Therapy. 2021; 12: 442. https://doi.org/10.1186/s13287-021-02528-x.
- [24] Rao F, Wang Y, Zhang D, Lu C, Cao Z, Sui J, *et al.* Aligned chitosan nanofiber hydrogel grafted with peptides mimicking bioactive brain-derived neurotrophic factor and vascular endothelial growth factor repair long-distance sciatic nerve defects in rats. Theranostics. 2020; 10: 1590–1603. https://doi.org/10.7150/thno.36272.

